Heliyon 10 (2024) e33899

Contents lists available at ScienceDirect

Heliyon

journal homepage: www.cell.com/heliyon

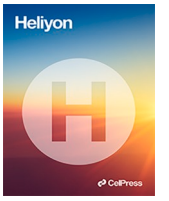

Research article

Establishment of a predictive model of CT value in the diagnosis and differential diagnosis of pulmonary cryptococcosis

Yajing Ning [a,b], Furong Meng [a,b,1], Hao Zhang [c,1], Wanjing Li [a,b], Zhangyan Ke [a,b], Fangzhou Xu [a,b], Yanbei Zhang [a,b,*]

[a] *Department of Geriatric Respiratory and Critical Care Medicine, the First Affiliated Hospital of Anhui Medical University, Hefei, Anhui Province, 230022, China*
[b] *Anhui Geriatric Institute, The First Affiliated Hospital of Medical Anhui Medical University, Hefei, Anhui Province, 230022, China*
[c] *Fuyang Second People's Hospital, Fuyang, Anhui Province, 236029, China*

ARTICLE INFO

Keywords:
Pulmonary cryptococcosis
Pulmonary space-occupying lesions
CT value
Prediction model

ABSTRACT

Objective: To investigate the application value of computed tomography (CT) value (HU) in the diagnosis and differential diagnosis of pulmonary cryptococcosis (PC) and to construct a prediction model.

Methods: Retrospective analysis of the clinical data of 73 patients who presented with nodular/mass-type occupations on lung CT and confirmed by histopathology in our hospital from January 2019 to May 2022 were divided into PC group (23 patients) and non-PC group (50 patients) according to the pathological findings, and the CT values of each patient's lung lesions were measured. The differences in age, gender, symptoms, lesion involvement in one/both lungs, lung lobe distribution, number of lesions, maximum lesion diameter (cm), lesion margin condition, and CT value results were compared between the two groups. Independent risk factors for PC were analyzed for indicators with statistically significant differences, clinical prediction models were constructed and column line plots were drawn, C (correction) indices were calculated, subject characteristics (ROC) curves were drawn, calibration curves and clinical decision curve analysis (DCA) were performed to further evaluate the predictive efficacy of the models.

Results: Comparative analysis of patient data between the two groups showed statistically significant differences in central, peripheral and global CT values ($P < 0.05$), and multiple regression analysis indicated that central CT value, peripheral CT value and global CT value could be used as independent risk factors for the diagnosis and differential diagnosis of PC. The area under the ROC curve of the model predicting PC was 0.814 (95 % CI: 0.7011–0.9267), and the corrected C-index (Bootstrap = 1000) was 0.781; the actual curve overlapped well with the calibration curve; the DCA results indicated that the column line graph model has high clinical application value.

Conclusions: CT value measurements of lesions can be used as an independent risk factor for PC, and clinical prediction models based on the above factors are predictive for the diagnosis and differential diagnosis of PC.

* Corresponding author. Department of Geriatric Respiratory and Critical Care Medicine, the First Affiliated Hospital of Anhui Medical University, Hefei, Anhui Province, 230022, China.
E-mail address: zhangyanbei1963@126.com (Y. Zhang).
[1] These authors contributed equally to this article.

https://doi.org/10.1016/j.heliyon.2024.e33899
Received 15 March 2024; Received in revised form 27 June 2024; Accepted 28 June 2024
Available online 29 June 2024

1. Introduce

Pulmonary cryptococcosis (PC) is a fungal infection that occurs after inhalation of Cryptococcus neoformans or Cryptococcus gattii spores, and is a chronic, subacute or acute fungal infection of the lung [1]. PC is an important opportunistic invasive fungal disease in immunocompromised patients, but it is also increasingly seen in immunocompetent patients [2].Due to the limitations of diagnostic tools, PC remains underdiagnosed [3], and its imaging presentation is often similar to that of pulmonary diseases such as bacterial pneumonia, lung cancer, tuberculosis and other pulmonary fungal diseases [4,5], Pulmonary lesions in patients with cryptococcal infections usually indolent and appears as a localized nodule or a mass [6,7].It may manifest as single nodules, multiple clustered nodules, multiple scattered nodules, or mass like or pneumonic opacity [8].Some other researches shows the common chest imaging of PC includes nodule, masses,consolidation,and pleural efusion [9–11].making its imaging presentation nonspecific. In addition,the insidious onset and complex clinical types make the diagnosis and differential diagnosis of PC more difficult and prone to misdiagnosis and omission [12]. In this paper, we mainly analyzed the clinical data of 73 patients retrospectively, measured the computed tomography (CT) value (HU) of pathologically confirmed lesions of different diseases, and constructed a prediction model, aiming to improve the diagnosis and differential diagnosis of PC and provide reference for early clinical diagnosis and treatment.

2. Data and methods

2.1. Sources of information

73 patients presenting with nodular/mass-type occupancy on CT of the lung in our hospital from January 2019 to May 2022 were selected and divided into PC group (23 patients) and non-PC group (50 patients) according to the patients' postoperative or biopsy pathological findings.The histopathological types of non-PC group include:pulmonary malformation tumor, pulmonary tuberculosis, pulmonary neoplasm, other inflammatory lesions(bacterial pneumonia, fungal infection other than PC.

2.2. Inclusion and exclusion criteria

Inclusion criteria: (1) all patients had a lung CT presentation showing an occupying lung lesion; (2) all patients underwent surgical resection or lung puncture biopsy with pathologically confirmed PC: a, cytopathology of the lung specimen finding cryptococci or cryptococcal spores; b, histopathology of the lung specimen showing granulomatous inflammation with positive special staining (silver hexamine stain and/or Schiff's periodate stain); or histopathology Confirmation of other types of pulmonary lesions: pulmonary malformation tumor; pulmonary tuberculosis; pulmonary neoplasm; other inflammatory lesions.

Exclusion criteria: (1) patients with HIV infection; (2) patients with previously treated pulmonary occupying lesions; (3) patients on

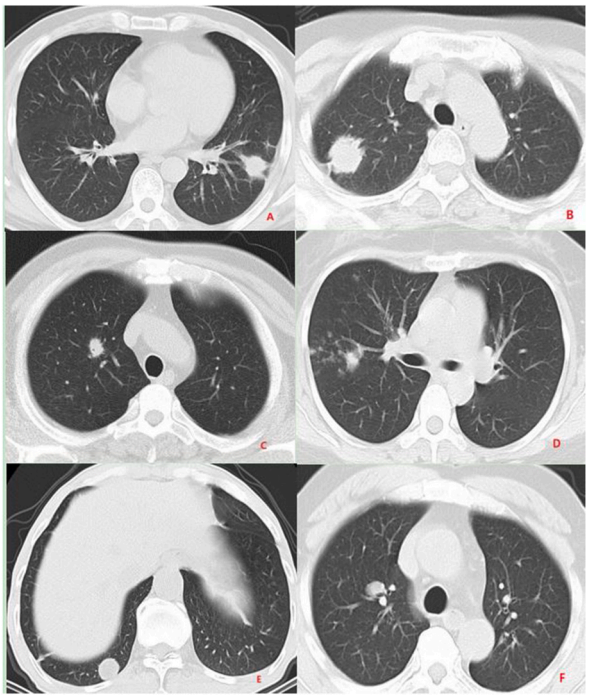

Fig. 1. Several different manifestations of pulmonary nodules, include PC(A),lung cancer (B),tuberculosis(C),pneumonia(D) and pulmonary hamartoma(E,F).

long-term immunosuppressive therapy; (4) those with incomplete data.

2.3. Instrumentation

A GE Optima CT 680 64-row spiral CT scanner was used. Scanning parameters: tube voltage 120 kV, tube current 300 mA, spiral scanning mode, pitch 1.2, CT scan of the patient's chest. The patients were scanned in the supine position, and the scan was started after inspiration, with a layer thickness and layer spacing of 5 mm from the lung tip to the rib-diaphragm angle. All images were observed and analyzed by two attending radiologists with many years of experience in film review to observe the distribution, morphology, density, and number of lesions (see Fig. 1).

The flowchart is shown in Fig. 2.

2.4. Research methods

The basic clinical data and radiological manifestations of 73 patients were retrospectively analyzed. The imaging manifestations included single and double lungs, lung lobe distribution, number of lesions, whether the lesion margins were shiny or not, and the maximum diameter of the lesions (the largest was selected for multiple lesions). The patient's lung CT was also accessed, and the central, peripheral, and global CT values of the lesions were measured (the largest was selected for multiple lesions). The peripheral CT values were selected as the average of the measured values of the upper, lower, left and right ends of the lesions(Fig. 3A), and the central and peripheral CT values were measured over an area of 4.80 mm^2–5.20 mm^2(Fig. 3B). The global CT values of irregular lesions were measured over a larger solid area if possible(Fig. 3C).Binary regression analysis of independent risk factors for PC was applied for statistically significant difference indicators. Clinical modeling was performed with the aid of R software and column plots were drawn, and the C (correction) index, receiver operating characteristic curve (ROC), calibration curve and clinical decision curve analysis (DCA) were calculated to further evaluate the predictive model performance.

2.5. Statistical methods

All data analysis and plots were completed using R 3.6.3 (http://www.R-project.org). Count data in terms of cases and rates were expressed using *Fisher's* exact probability method or χ^2-test; measures with normal distribution in ($\bar{\chi} \pm s$) were expressed using independent samples *t*-test; measures that did not conform to normal distribution were expressed using M (P25, P75) and *Mann-Whitney U test* was applied. Differences were considered statistically significant at $P < 0.05$. The regression model with minimum AIC was

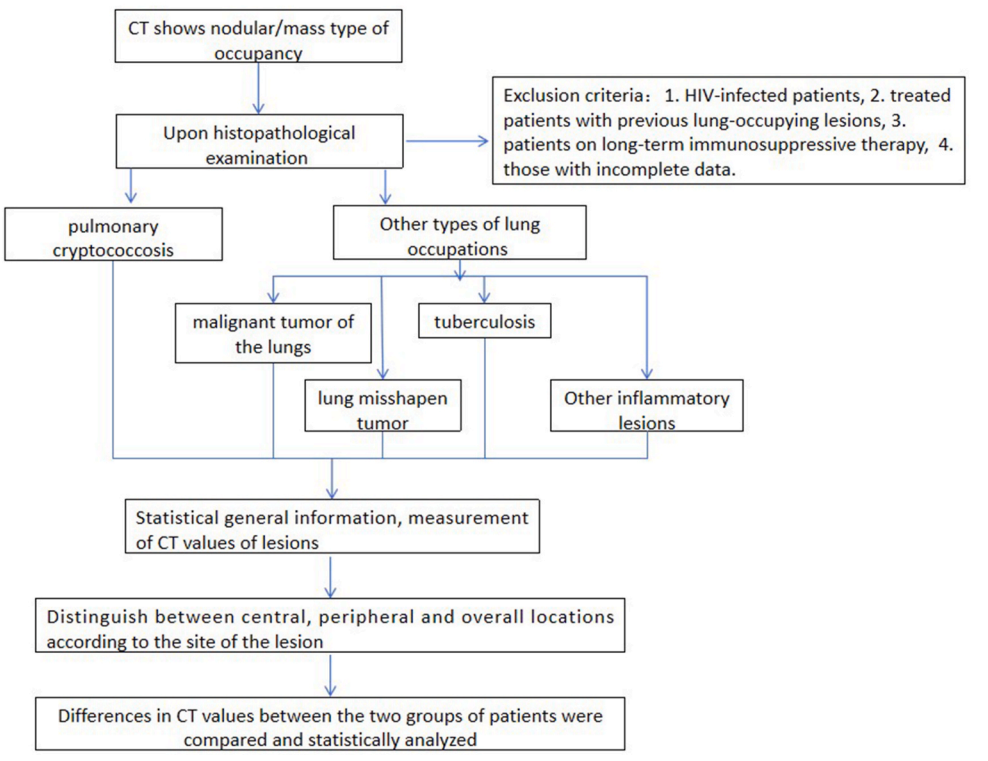

Fig. 2. The flowchart for patients inclusion.

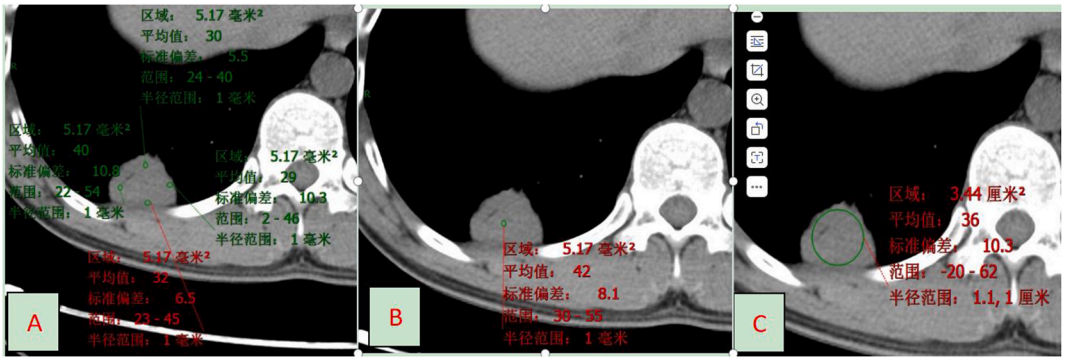

Fig. 3. the method of measuring CT value,the peripheral CT values were selected as the average of the measured values of the upper, lower, left and right ends of the lesions(A), the central and peripheral CT values were measured over an area of 4.80mm2–5.20mm2(B). The global CT values of irregular lesions were measured over a larger solid area if possible(C).

obtained by screening variables through logistic stepwise regression analysis of all independent variables using the MASS package in R software. Further to apply the R software rms package to the above independent risk factors row PC diagnosis of risk factors column line plot. Bootstrap resampling method (set B = 1000) was applied for internal validation of the model. The C-index, corrected C-index and area under curve (AUC) were further calculated according to the prediction model to evaluate the predictive efficacy of the prediction model, and DCA was applied to evaluate the clinical applicability of the prediction model for PC diagnosis, and the corrected, ROC and clinical decision curves of the prediction model were also produced.

3. Results

3.1. Comparison of general data between the two groups of patients

The results of the comparison of the underlying data between the two groups are shown in Table 1, which indicates that the difference in CT value measurements of lesions between the two groups is statistically significant ($P < 0.05$).

Table 1
Comparison of various clinical factors of PC and non-PC.

Variable	Non-PC	PC	Standardize diff	*P*-values
Number	50	23		
Age	55.80 ± 12.68	50.91 ± 13.46	0.37 (−0.12, 0.87)	0.138
Maximum diameter of lesion	30.67 ± 20.99	26.91 ± 15.21	0.20 (−0.29, 0.70)	0.444
Central CT value	30.75 ± 13.69	50.27 ± 34.64	0.74 (0.23, 1.25)	<0.001
Peripheral CT value	59.71 ± 23.56	101.44 ± 50.17	1.06 (0.54, 1.59)	<0.001
Global CT value	22.76 ± 16.26	38.36 ± 33.72	0.59 (0.09, 1.09)	0.009
Gender			0.24 (−0.25, 0.74)	0.345
Female	21 (42.00 %)	7 (30.43 %)		
Male	29 (58.00 %)	16 (69.57 %)		
Symptoms			0.14 (−0.36, 0.63)	0.583
No	23 (46.00 %)	9 (39.13 %)		
Yes	27 (54.00 %)	14 (60.87 %)		
Lung's side			0.43 (−0.07, 0.92)	0.257
Left	9 (18.00 %)	7 (30.43 %)		
Right	16 (32.00 %)	9 (39.13 %)		
Double	25 (50.00 %)	7 (30.43 %)		
Distribution of lung			0.39 (−0.11, 0.89)	0.489
Upper lobe of the lung	15 (30.00 %)	6 (26.09 %)		
Middle lobe of the lung	1 (2.00 %)	1 (4.35 %)		
Lower lobe of the lung	10 (20.00 %)	8 (34.78 %)		
Multilobar lung	24 (48.00 %)	8 (34.78 %)		
Number of lesions			0.00 (−0.49, 0.50)	0.994
Single	13 (26.00 %)	6 (26.09 %)		
Multiple	37 (74.00 %)	17 (73.91 %)		
Lesion margin			0.05 (−0.44, 0.54)	0.841
Smooth	23 (46.00 %)	10 (43.48 %)		
Rough	27 (54.00 %)	13 (56.52 %)		

3.2. Univariate analysis

In the analysis for each clinical index, the results showed that the CT value measurement of the lesion was an influential factor in differentiating PC from other pulmonary lesions. Each specific result is shown in Table 2.

3.3. Multiple regression analysis

Multiple regression analysis was performed with central CT value, peripheral CT value, and global CT value as independent variables and whether the lesion was PC as dependent variable. In model I, the adjusted variables were age and sex, and in model II, the adjusted variables were age, gender, lung's side, lobe, symptoms, lesion margin condition, number of lesions, and maximum diameter of lesions, and the results showed that focal CT value measurements could be used as an independent risk factor for PC. As shown in Table 3.

3.4. Clinical prediction model construction

According to the results of multiple regression analysis, high CT values in the center, periphery and the whole lesion are independent risk factors for PC. This risk factor was plotted as a nomogram (Fig. 4).

3.5. Prediction model evaluation

The model correction by calculation and using Bootstrap resampling method (B = 1000) yielded a corrected C-index of 0.781. The ROC analysis suggested that the area under the curve was 0.814 (95 % CI: 0.7011–0.9267), suggesting that the CT value was a good predictor of the diagnosis of PC, as shown in Fig. 5. The corrected curve by Bootstrap resampling method still overlaps well with the actual curve, as shown in Fig. 6.

3.6. Decision curve analysis

The clinical applicability of the PC diagnostic prediction model was evaluated using DCA, where the horizontal line indicates that all samples are negative and the net benefit is 0, and the diagonal line indicates that all samples are positive and the net benefit is an inverse slope with a negative slope. The farther the decision curve is from the 2 extreme lines, the higher the value of the clinical application of the column line diagram, as shown in *Fig. 7*. The results of DCA indicate that the column line diagram model can improve the predictive ability of PC within a large range of risk threshold probabilities.

Table 2
Univariate analysis of clinical factors influencing PC.

	Statistics	OR (95 % CI)	*P*-value
Age	54.26 ± 13.04	0.97 (0.93, 1.01)	0.1391
Gender			
Female	28 (38.36 %)	1.0	
Male	45 (61.64 %)	1.66 (0.58, 4.73)	0.3473
Symptoms			
No	32 (43.84 %)	1.0	
Yes	41 (56.16 %)	1.33 (0.48, 3.62)	0.5831
Lung's side			
Left	16 (21.92 %)	1.0	
Right	25 (34.25 %)	0.72 (0.20, 2.61)	0.6202
Double	32 (43.84 %)	0.36 (0.10, 1.31)	0.1222
Distribution of lung			
Upper lobe of the lung	21 (28.77 %)	1.0	
Middle lobe of the lung	2 (2.74 %)	2.50 (0.13, 46.78)	0.5398
Lower lobe of the lung	18 (24.66 %)	2.00 (0.53, 7.54)	0.3059
Multilobar lung	32 (43.84 %)	0.83 (0.24, 2.88)	0.7731
Number of lesions			
Single	19 (26.03 %)	1.0	
Multiple	54 (73.97 %)	1.00 (0.32, 3.07)	0.9937
Lesion margin			
Smooth	33 (45.21 %)	1.0	
Rough	40 (54.79 %)	1.11 (0.41, 2.99)	0.8406
Maximum diameter of lesion	29.48 ± 19.33	0.99 (0.96, 1.02)	0.4413
Central CT value	36.90 ± 24.03	1.04 (1.01, 1.07)	0.0049
Peripheral CT value	72.86 ± 39.09	1.04 (1.02, 1.07)	0.0003
Global CT value	27.67 ± 24.10	1.03 (1.00, 1.06)	0.0208

Table 3
Multiple regression analysis of clinical factors affecting PC.

	Unadjusted		Model I		Model II	
	OR (95 % CI)	***P*-value**	**OR (95 % CI)**	***P*-value**	**OR(95 % CI)**	***P*-value**
Central CT value	1.04(1.01, 1.07)	0.0049	1.04 (1.01, 1.07)	0.0079	1.04(1.01, 1.07)	0.0086
Peripheral CT value	1.04(1.02, 1.07)	0.0003	1.04 (1.02, 1.07)	0.0007	1.04(1.02, 1.07)	0.0012
Global CT value	1.03(1.00, 1.06)	0.0208	1.03 (1.01, 1.06)	0.0100	1.04(1.01, 1.08)	0.0088

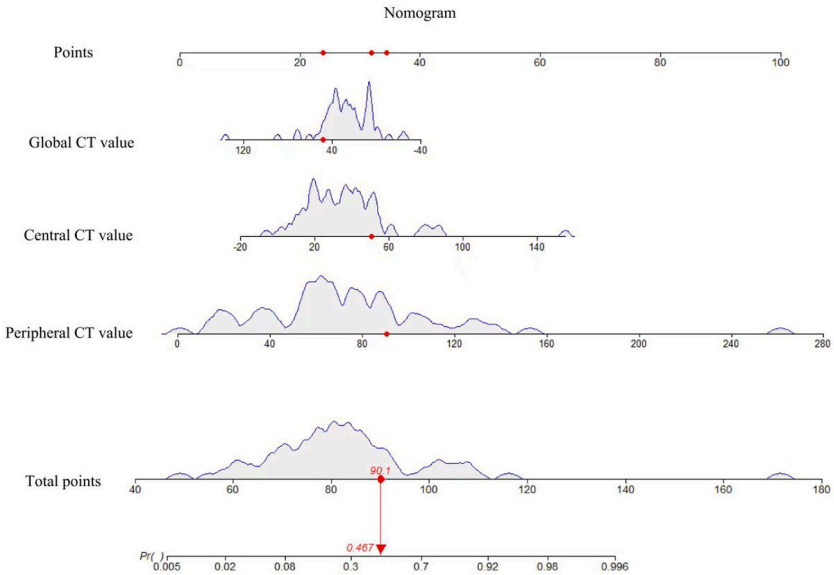

Fig. 4. Nomogram of CT measurements for risk prediction of PC.

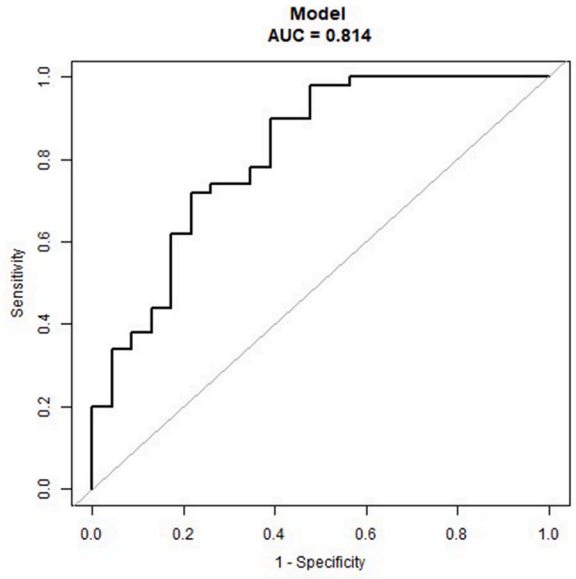

Fig. 5. Nomo prediction model for CT value results for PC diagnosis risk prediction.

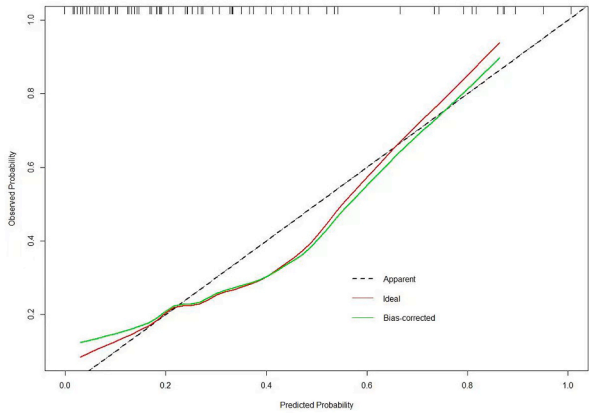

Fig. 6. Calibration curve by Bootstrap resampling method (set B = 1000).

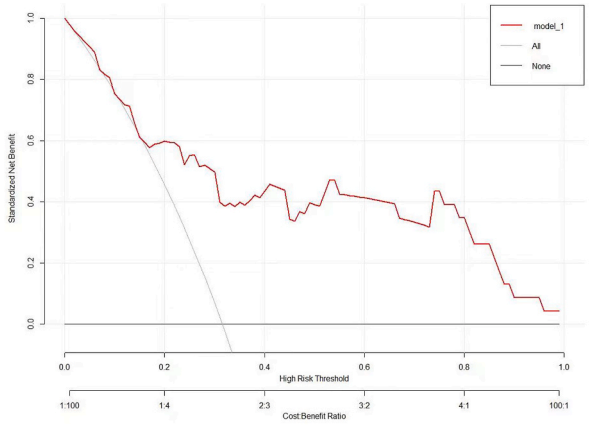

Fig. 7. DCA analysis of CT value on PC diagnostic prediction model.

4. Discuss

PC is a fungal infection of the lungs second only to pulmonary aspergillosis and is caused by infection with Cryptococcus neoformans, with a probability of occurrence of about 20 %[13]. Given its insidious onset, atypical symptoms, and diverse imaging manifestations, the diagnosis and differential diagnosis are difficult. The nodule/mass pattern is the most common CT manifestation and is often confused with other imaging manifestations of lung-occupying lesions. The diagnosis of pulmonary histopathology is still the gold standard, but for some patients who cannot undergo pulmonary histopathology, it is crucial to use a combined multi-information model to make the further diagnosis of pulmonary occupying lesions. With the improvement of CT thin-layer scanning technology, increasingly higher image resolution can be obtained, and the density of the lesion on CT can reflect some extent the growth of tissue cells within the lesion. There have been many studies on the use of CT values to determine the nature of pulmonary ground-glass nodules [14–16], but there are few studies on the application of CT values in other pulmonary space-occupying lesions. Relevant studies have shown that the average lung density method, that is, the CT value can reflect the comprehensive density of lung parenchyma, gas, tissue fluid, interstitial and blood, and provide data for the quantitative analysis of the distribution of lesions [17]. The CT value can quantitatively reflect the average density of tissues in the selected area, and changes in the content of chemical substances, blood flow and any cellular structure in the local tissue can make the CT value change. Therefore, it can also be considered as a direct reflection of pathological changes in regional tissues.

In the present study, comparing the general data and imaging characteristics of PC patients and non-PC patients, the results showed no significant difference, which also indicates that CT, as a common radiological examination for chest diseases, although it has an important role in the diagnosis and differentiation of lung diseases, it is difficult to give an accurate judgment due to the lack of specificity in the imaging presentation of PC. In comparing the results of central CT values, peripheral CT values and global CT values obtained from the two groups of patients, differences were found ($P < 0.05$), indicating that the CT value measurements might provide a reference for the differential diagnosis of PC and other types of pulmonary occupying lesions.

The content of solid components in the lesion can be reflected by CT value. Combined with the results of this study, the larger the CT value, the more likely the disease nature was to be PC ($P < 0.05$), which may be related to the fact that the PC showed more masses or

solid nodules on imaging. Studies have shown that masses/solitary nodules are the most common imaging findings of PC [18]. First, PC pathogens are deposited in the lower lung due to gravity; second, it will spread along the blood stream and migrate to the end of the pulmonary circulation where the blood flow is slow or stagnant [19]. In addition, because cryptococcus mostly has a capsule, its capsule can be combined with IgG, and the complex formed by the combination of the capsule and IgG can be combined with the cR (FcRI and FcRIII) of phagocytes via the Fc segment of IgG, thus inducing phagocytosis and clearance of antigen-antibody complexes by phagocytes [20]. Phagocytes phagocytose PC pathogens and form fibrous tissues and inflammatory granulomas with lymphocytes, tissues and fibrocytes, thus limiting the spread of PC [21]. And most of the PC are low inflammatory response or granulomatous inflammation, while the general inflammatory response from infection causes capillary dilation and more scattered distribution of lesions, and lung cancer is mostly due to tumor vascular formation, therefore, compared to other nature of lesions, the solid component of lesions in PC is higher and higher than other lesions in CT value measurement results.

The results of data analysis in this study showed that the central CT value, peripheral CT value and global CT value obtained from lesion measurement could be used as independent risk factors for PC patients compared with other lung occupying lesions. The Nomo prediction model was constructed on this basis, and the area under the ROC curve of the nomogram was 0.814 (95%CI: 0.7011–0.9267). After correction, C-index was 0.781. The actual curve overlaps well with the calibrated curve. It indicates that the model prediction has high application value in clinical practice. The results of DCA curve showed that the nomogram model had certain clinical application value. Therefore, for patients with lung space occupying lesions who are not suitable for lung histopathology examination, it is beneficial to the diagnosis and differential diagnosis of PC by observing the imaging manifestations of the lesions and combining the CT value measurement results of multiple parts of the lesions,and also has the advantages of easy operation and non-invasive.

The limitations of this paper are: 1.The PC group selection criteria: in this study, the PC group includes a variety of lung space space-occupying lesions, such as lung cancer, benign tumor, tuberculosis and other inflammatory lesions. These cases were all confirmed by histopathology. Though these lesions have heterogeneity to some extent, but we do realize that encountered in the clinical practice group of patients may be more complicated and varied. 2.Preliminary Nature of the study: The aim of this study was to preliminarily explore the application value of CT value in the diagnosis of pulmonary cryptococcosis. Although the selection of the non-PC group may have simplified the problem to some extent, preliminary findings have shown the potential of CT value as a diagnostic index. We believe that this is an important starting point for further expansion of future research.

Future research improvements:Diverse non-PC group: In future studies, we plan to include a more diverse group of non-PC cases, covering a wider spectrum of lung diseases. This will include more complex cases, such as patients with multiple combined lesions, to improve the applicability of the model for practical clinical applications.Multi-center cooperation: By cooperating with more medical institutions to collect data from patients with different types of lung diseases in different regions, we can ensure that the results of our study have wider application and promotion value.Although preliminary model validation and optimization: existing research showed the potential of CT value in the diagnosis of PC, but we are planning in a follow-up study, through the larger samples and more complex data validation and optimization of the model. This will involve advanced data analysis methods, such as machine learning, and more diverse clinical and radiographic features, in order to improve the diagnostic accuracy and reliability of the model.

5. Conclusion

In conclusion, the CT value measurement results of this study can be used as an independent risk factor for PC, which is helpful to differentiate it from other pulmonary space occupying diseases, and can help clinicians to diagnose and differentiate PC as early as possible. However, it is worth noting that lung histopathology is still the most recommended approach to avoid missed diagnosis of lung malignancies.

Ethics approval and informed consent

This study was approved by the Clinical Medical Research Ethics Committee of the First Affiliated Hospital of Anhui Medical University (number PJ20231148). The requirement for written informed consent was waived due to the retrospective nature of the study. All data used in this manuscript were anonymized.

Data availability statement

The data associated with this study has not been deposited into a publicly available repository,but it will be made available on request.

Funding

This research did not receive any specific funding.

CRediT authorship contribution statement

Yajing Ning: Writing – original draft. **Furong Meng:** Data curation. **Hao Zhang:** Formal analysis. **Wanjing Li:** Methodology. **Zhangyan Ke:** Formal analysis. **Fangzhou Xu:** Resources. **Yanbei Zhang:** Writing – review & editing.

Declaration of competing interest

The authors declare that they have no known competing financial interests or personal relationships that could have appeared to influence the work reported in this paper.

Acknowledgments

We would like to acknowledge Dr. Yanbei Zhang for her kind assistance with language editing.

References

[1] X. Sui, Y. Huang, W. Song, et al., Clinical features of pulmonary cryptococcosis in thin-section CT in immunocompetent and non-AIDS immunocompromised patients, Radiol. Med. 125 (1) (2020) 31–38, https://doi.org/10.1007/s11547-019-01088-8.
[2] F. Setianingrum, R. Rautemaa-Richardson, D.W. Denning, Pulmonary cryptococcosis: a review of pathobiology and clinical aspects, Med. Mycol. 57 (2) (2019) 133–150, https://doi.org/10.1093/mmy/myy086.
[3] D. Yamamura, J. Xu, Update on pulmonary cryptococcosis, Mycopathologia 186 (5) (2021) 717–728, https://doi.org/10.1007/s11046-021-00575-9.
[4] H.W. Choi, S. Chong, M.K. Kim, I.W. Park, Pulmonary cryptococcosis manifesting as diffuse air-space consolidations in an immunocompetent patient, J. Thorac. Dis. 9 (2) (2017) E138–E141, https://doi.org/10.21037/jtd.2017.02.11.
[5] S. Zheng, T.T. Tan, J.M.F. Chien, Cryptococcus gattii infection presenting as an aggressive lung mass, Mycopathologia 183 (3) (2018) 597–602, https://doi.org/10.1007/s11046-017-0233-6.
[6] J.A. Aberg, L.M. Mundy, W.G. Powderly, Pulmonary cryptococcosis in patients without HIV infection, Chest 115 (1999) 734–740, https://doi.org/10.1378/chest.115.3.734.
[7] W.C. Chang, C. Tzao, H.H. Hsu, et al., Pulmonary cryptococcosis: comparison of clinical and radiographic characteristics in immunocompetent and immunocompromised patients, Chest 129 (2006) 333–340, https://doi.org/10.1378/chest.129.2.333.
[8] S. Murayama, S. Sakai, H. Soeda, et al., Pulmonary cryptococcosis in immunocompetent patients: HRCT characteristics, Clin. Imag. 28 (2004) 191–195, https://doi.org/10.1016/S0899-7071(03)00145-1.
[9] Y. Zhang, N. Li, Y. Zhang, H. Li, X. Chen, S. Wang, et al., Clinical analysis of 76 patients pathologically diagnosed with pulmonary cryptococcosis, Eur. Respir. J. 40 (2012) 1191–1200.
[10] J.Q. Yu, K.J. Tang, B.L. Xu, C.M. Xie, R.W. Light, Pulmonary cryptococcosis in non-AIDS patients, Braz. J. Infect. Dis. 16 (2012) 531–539.
[11] S.E. Zinck, A.N. Leung, M. Frost, G.J. Berry, N.L. Müller, Pulmonary cryptococcosis: CT and pathologic fndings, J. Comput. Assist. Tomogr. 26 (2002) 330–334.
[12] L.A. Chen, D.Y. She, Z.X. Liang, et al., A prospective multi-center clinical investigation of HIV-negative pulmonary cryptococcosis in China [J], Chin. J. Tuberc. Respir. Dis. 44 (1) (2021) 14–27, https://doi.org/10.3760/cma.j.cn112147-20200122-00034.
[13] T.F. Lai, C.Q. Chu, Y.L. Lin, et al., Correlation study of clinical features of pulmonary cryptococcosis with chest CT manifestations[J], Journal of Practical Radiology 36 (6) (2020) 897–900, https://doi.org/10.3969/j.issn.1002-1671.2020.06.011.
[14] S.H. Bak, H.Y. Lee, J.H. Kim, et al., Quantitative CT scanning analysis of pure ground-glass opacity nodules predicts further CT scanning change, Chest 149 (1) (2016) 180–191, https://doi.org/10.1378/chest.15-0034.
[15] S.H. Dai, G.F. Liu, D.S. Xiang, The significance of CT value measurement of pulmonary ground glass nodules in early cancer diagnosis[J], Chinese Journal of Lung Diseases 12 (6) (2019) 770–771, https://doi.org/10.3877/cma.j.issn.1674-6902.2019.06.024.
[16] A. Kitami, Y. Kamio, S. Hayashi, et al., One-dimensional mean computed tomography value evaluation of ground-glass opacity on high-resolution images, Gen Thorac Cardiovasc Surg 60 (7) (2012) 425–430, https://doi.org/10.1007/s11748-012-0066-7.
[17] W.W. Labaki, C.H. Martinez, F.J. Martinez, et al., The role of chest computed tomography in the evaluation and management of the patient with chronic obstructive pulmonary disease, Am. J. Respir. Crit. Care Med. 196 (11) (2017) 1372–1379, https://doi.org/10.1164/rccm.201703-0451PP.
[18] N.Y. Zeng, Y.H. Xu, J.L. Kong, et al., Clinical characteristics analysis of pulmonary cryptococcosis in patients with different immune status[J], Chinese Journal of Nosocomiology 26 (10) (2016) 2223–2226, https://doi.org/10.11816/cn.ni.2016-152492.
[19] D. Wang, C. Wu, J. Gao, et al., Comparative study of primary pulmonary cryptococcosis with multiple nodules or masses by CT and pathology, Exp. Ther. Med. 16 (6) (2018) 4437–4444, https://doi.org/10.3892/etm.2018.6745.
[20] O. Zaragoza, C.P. Taborda, A. Casadevall, The efficacy of complement-mediated phagocytosis of Cryptococcus neoformans is dependent on the location of C3 in the polysaccharide capsule and involves both direct and indirect C3-mediated interactions, Eur. J. Immunol. 33 (7) (2003) 1957–1967, https://doi.org/10.1002/eji.200323848.
[21] Y. Huang, X. Sui, L. Song, et al., Imaging manifestations of pulmonary cryptococcosis [J], Chin. Med. Sci. J. 41 (6) (2019) 832–836, https://doi.org/10.3881/j.issn.1000-503X.10985.